Study on the Production of Flaky Amorphous Alloy Powders by Impact Flattening of Atomized Liquid Droplets on a Rapidly Rotating Wheel

Study on the Production of Flaky Amorphous Alloy Powders by Impact Flattening of Atomized Liquid Droplets on a Rapidly Rotating Wheel*

Akihisa Inoue, Masahiro Oguchi+ and Tsuyoshi Masumoto

Institute for Materials Research

(Received December 28, 1992)

Synopsis

A two-stage quenching technique consisting of impact flattening of atomized supercooled liquid droplets caused the production of flaky amorphous powders with a thickness of 1 to 3 μm and an aspect ratio of 20 to 300 in Co-, Fe- and Al-based systems. The flaky powders consist of an amorphous phase over the entire particle size range even in the alloy systems where no amorphous phase is formed in the particle size below 25 μm by high-pressure gas atomization. The improvement of the production ratio of the amorphous powders is due to the following three factors; (1) the second-stage cooling of supercooled liquid droplets, (2) the reduction of powder thickness to 1 to 3 μm, and (3) the high thermal conductive state between rotator and powder resulting from the high-energy collision. The flaky powders also have smooth surface and edge combined with a uniform thickness, leading to good luster, high reflection ratio against light, high corrosion resistance, high mechanical strength and anisotropic magnetic properties. Furthermore, the unique morphology causes a high laminating tendency in a resin. By utilizing these advantages, the flaky amorphous powders are expected to be used as magnetic filler and corrosion-resistant coating materials.

I. Previous Techniques of Producing Amorphous Alloy Powders and Their Disadvantage Points

---

* The 1914th report of Institute for Materials Research.

+ Teikoku Piston Ring Co. Ltd., 2-1-13 Shinmei-cho, Okaya 394.

As the methods by which amorphous alloy powders are produced directly from melt, one can list up ultrasonic gas atomization[1], water atomization[2], high-pressure gas atomization[3], roller cavitation[4] and in-rotating liquid ejection[5] etc. In these techniques, the methods which enable the mass production of amorphous alloy powders with clean outer surface are limited to the ultrasonic gas atomization and high-pressure gas atomization. Since 1985, the present authors have carried out systematic studies on the development of high-pressure gas atomization which enables the production of amorphous alloy powders at high production ratios as well as on the clarification of alloy systems in which amorphous alloy powders are obtained and the morphology, structure and fundamental properties of the resulting powders. As a result, it has been clarified[3] that the average particle size and cooling rate of alloy powders obtained at atomizing pressures above about 7 MPa by the high-pressure gas atomization are nearly the same as those[1] for the ultrasonic gas atomization in the case of the same atomizing gas. It has subsequently been reported[3] that the average particle size of alloy powders obtained by high-pressure argon atomization is about 40 to 50 μm for important engineering alloys of $Fe_{77}P_{10}C_{13}$, $Fe_{75}Si_{10}B_{15}$ and $Co_{75}Si_{10}B_{15}$ etc. and the maximum diameter for the formation of an amorphous single phase is 25 μm for the Fe-P-C and Co-Si-B alloys and 38 μm for the Fe-Si-B alloy. This result indicates that the weight fraction for the formation of amorphous alloy powders in the high-pressure argon atomization is below 50 %. Accordingly, the development of new techniques in which the weight fraction for the formation of amorphous alloy powders increases significantly even in the argon or nitrogen atomization without the use of helium had strongly been desired for the practical use of amorphous alloy powders as engineering materials. With the aim of satisfying the above-described requirement, the study had been carried out[6-10] on the production of amorphous alloy powders by impact flattening of atomized liquid droplets on a rapidly rotating wheel. The basic concept of the new production technique is due to the achievement of a supercooled liquid quenching (a two-stage liquid quenching). This paper is intended to present the following points; (1) a basic principle of the new supercooled liquid quenching method, (2) an equipment which was constructed based on the new concept, (3) features of morphology and structure of the resulting amorphous powders, (4) a drastic increase in the production ratio of amorphous alloy powders caused by the significant increase of cooling rate, and (5) some examples of practical use for the amorphous alloy powders produced by the new

technique.

II. Supercooled Liquid Quenching Technique and its Advantage Points

In order to understand the feature of the supercooled liquid quenching technique, it is important to clarify the dominant factors for the cooling rate of small liquid droplets produced by high-pressure gas atomization of liquid which was heated at temperatures above melting temperature. It is known that the cooling rate of the powders increases with an increase of the heat-transfer coefficient and temperature difference between liquid and atomizing gas and with a decrease of the density and specific heat of liquid and the diameter of liquid droplets. In the case where the kind of atomizing gas, atomizing pressure, the temperature of liquid at ejecting time and alloy composition are constant, the size of liquid droplets (D_p) is a dominant factor for cooling rate. D_p can be expressed by the following equation[11];

$$D_p = D_o k_c [\eta_{melt}/\eta_{gas}(1+J_{melt}/J_{gas})]^{1/2}.$$

Here, D_o is the diameter of a molten metal stream, k_c a constant, η_{melt} the viscosity of molten metal, η_{gas} the dymanic viscosity of atomizing gas, J_{melt} the velocity of molten alloy and J_{gas} the velocity of atomizing gas. When the kind and gas pressure of atomizing gas and the temperature of molten alloy at the ejecting time are constant, the above-described equation indicates that D_p decreases with decreasing D_o and J_{melt}/J_{gas}. That is, the decrease in the diameter of molten alloy stream and the velocity of molten alloy as well as the increase in the amount of atomizing gas is effectve for the decrease in D_p. However, there is an anxious point that the decrease in the stream diameter and melt velocity causes the interuption of the falling of the molten alloy. In addition, the significant increase in the amount of atomizing gas is not always easy from the limitation of atomizing gas pressure. Thus, the above-described equation indicates that the increase in cooling rate of atomized powders has an upper limit in the high-pressure gas atomization technique. Consequently, the critical powder size for the formation of an amorphous single phase is presumed to result from the upper limit.

As a method to eliminate the upper limit, the present authors paid attention to the point that small liquid droplets obtained by high-pressure gas atomization with an atomizing pressure above 7 MPa

have high flight velocities ranging from 200 to 1000 m/s[12]. That is, it is expected that a significantly improved cooling velocity is obtained through the impact flattening of atomized liquid droplets onto a rapidly rotating wheel. Figure 1 shows the difference of the concepts between the supercooled liquid quenching method and the conventional liquid quenching method. Furthermore, Fig. 2 shows a schematic diagram illustrating the possibility that all powders can be

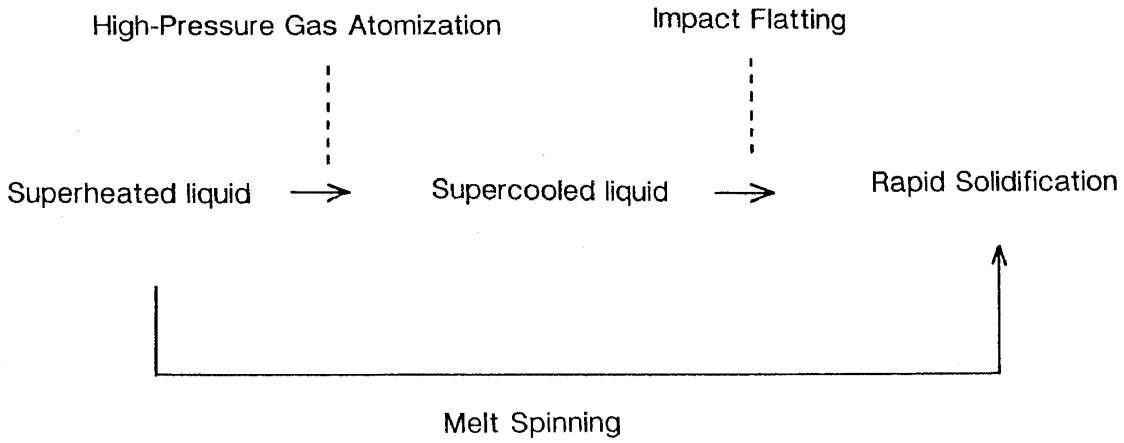

Fig. 1 Concept of a supercooled liquid (two-stage) quenching process in comparison with that for a conventional liquid quenching process.

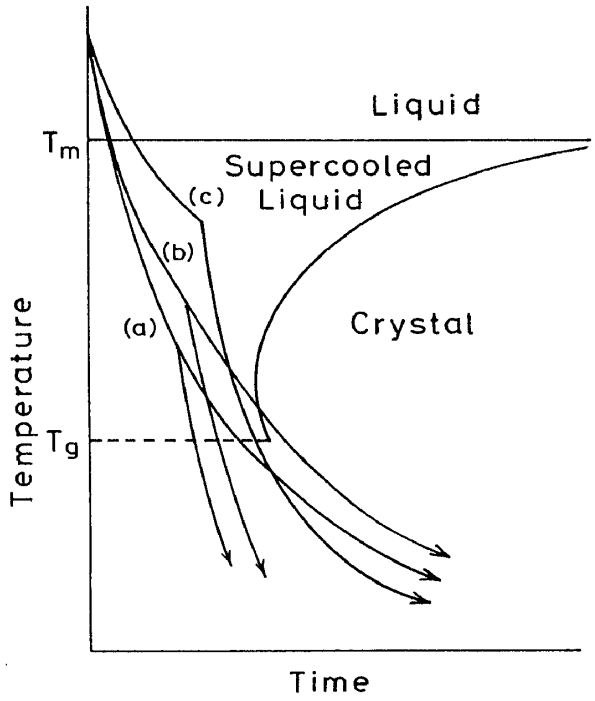

Fig. 2
Schematic illustration showing effect on a second-stage cooling on the increase in cooling rate in the supercooled liquid quenching process.

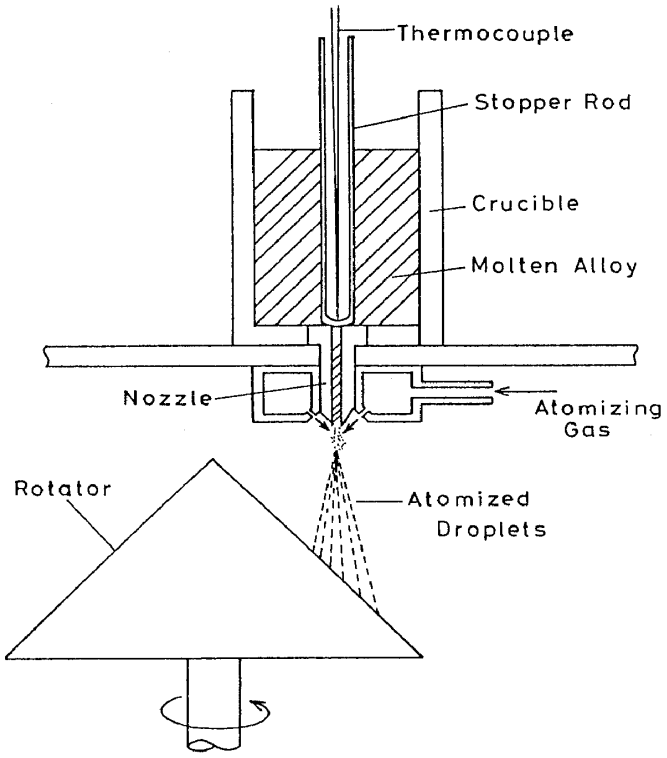

Fig. 3
Schematic illustration of a two-stage quenching equipment incorporating high-pressure gas atomization and centrifugal spinning.

amorphized through the increase in cooling rate resulting from the impact flattening of supercooled liquid droplets on the second-stage cooling medium. Figure 3 shows a schematic illustration of the main parts of a newly designed equipment which enables the second-stage quenching of supercooled liquid droplets. The molten stream heated at temperatures above T_m is atomized to small liquid droplets with temperatures below T_m by high dynamic pressure and the resulting liquid droplets have high flight velocities ranging from 200 to 1000 m/s. As a result, the small supercooled liquid droplets impinge at high kinetic energies against a cone rotator which is rotating at a high velocity of 7000 rpm at a position which is 150 mm away from the nozzle, followed by flattening and then solidification. As an example, Fig. 4 shows the morphology of the $Fe_{69}Cr_8P_{13}C_{10}$ powders with different particle sizes produced by the supercooled liquid quenching method. It is to be noticed that the powder morphology is significantly different from the spherical and falky morphologies obtained by the conventional gas atomization and the roller cavitation method, respectively. As shown in Fig. 5, the feature of the morphology for the resulting powders is summarized as follows; (1) the thickness is as small as 1 to 3 μm and uniform, (2) the shape is an

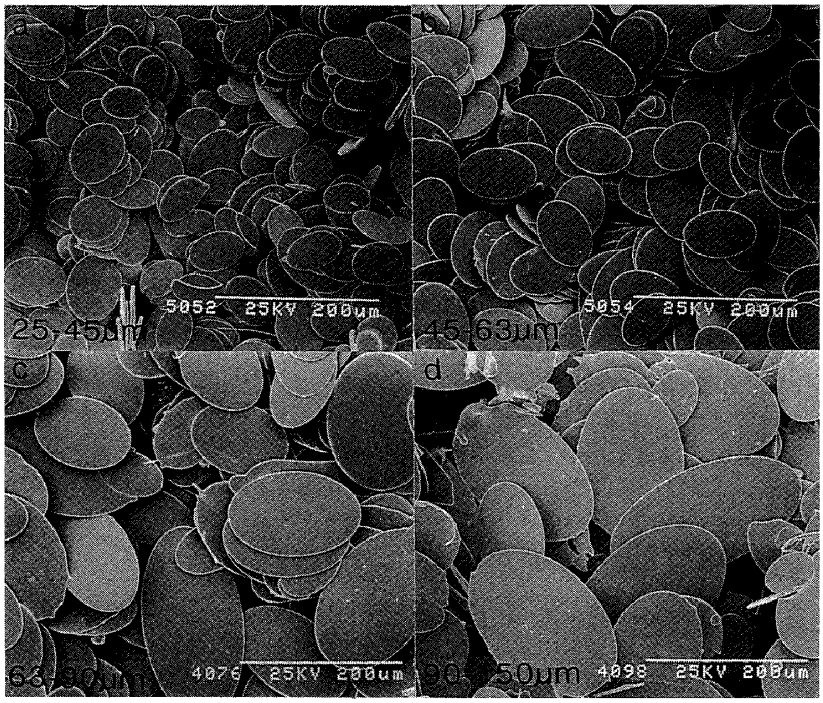

Fig. 4 Scanning electron micrographs showing the morphology of flaky $Fe_{69}Cr_8P_{13}C_{10}$ amorphous powders produced by the two-stage quenching method.

Alloy	t (μm)	w (μm)	l/w	Aspect ratio l/t	Property
$Co_{70.5}Fe_{4.5}Si_{10}B_{15}$	1-3	25-150	1.1-2.5	20-300	Soft magnetism
$Fe_{69}Cr_8P_{13}C_{10}$	1-3	25-150	1.1-2.6	20-300	High corosion resistance
$Al_{84}Ni_{10}Mm_6$	1-3	25-150	1.2-4.0	20-300	High luster High corrosion resistance

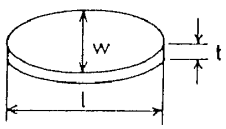

Fig. 5 Morphology and properties of flaky amorphous $Co_{70.5}Fe_{4.5}Si_{10}B_{15}$, $Fe_{69}Cr_8P_{13}C_{10}$ and $Al_{84}Ni_{10}Mm_6$ powders produced by the two-stage quenching method.

oval with large aspect ratios of 20 to 300, and (3) the surface is very smooth and the edge is sharp. Figure 6 shows the X-ray diffraction patterns taken from the flaky $Co_{70.5}Fe_{4.5}Si_{10}B_{15}$ powders with different particle sizes. All the powders consist only of an amorphous single, being significantly different from the previous result[3] that the spherical powders obtained by high-pressure gas atomizaion have an amorphous structure only in the particle size fraction below 25 μm. It is to be noticed that the use of the supercooled liquid quenching technique enables the production of amorphous powders over the whole particle size fractions.

In the new process leading to the second-stage cooling of supercooled liquid droplets produced by high-pressure atomization, it is expected that the cooling rate of the liquid droplets in the temperature range below T_g increases significantly as compared with those for high-pressure (or ultrasonic) gas atomization and single-roller type melt spinning, as illustrated in Fig. 2. In order to examine the difference in cooling rate in the temperature range below T_g between the flaky amorphous powder and the melt-spun ribbon with 20 μm in thickness, the structural relaxation behavior upon continuous heating was measured by DSC. Figure 7 shows the temperature dependence of apparent specific heat (C_p) for the falky powder and the ribbon of a $Co_{70.5}Fe_{4.5}Si_{10}B_{15}$ alloy heated at 0.67 K/s. Here, $C_{p,q}$ and $C_{p,s}$ represent the C_p values of the as-quenched state and the annealed state for 60 s at 800 K, respectively. The exothermic amount (ΔH_r) which is defined by $\int \Delta C_p dT$, $\Delta C_p (=C_{p,s} - C_{p,q}) > 0$ corresponds to the structural relaxation of the as-quenched sample which occurs during continuous heating and there is a clear tendency for ΔH_r to increase with increasing cooling rate of the sample during rapid solidification. As shown in Fig. 7, in comparison with that for the melt-spun ribbon, the structural relaxation of the flaky powder begins to occur at a lower temperature and the ΔH_r is considerably larger over the entire temperature range. ΔH_r is 1.84 kJ/mol for the 25-37 μm powder, 1.77 kJ/mol for the 74-88 μm powder and 0.66 kJ/mol for the ribbon. These distinct differences imply that the flaky powder was cooled at a much higher cooling rate in the temperature range between T_g and room temperature as compared with that for the ribbon, indicating the appropriateness of the schematic illustration shown in Fig. 2. The reason for the achievement of the larger cooling rate for the present process than for the single-roller melt spinning and the high-pressure gas atomization is presumed to originate from the simultaneous satisfaction of the following factors; (1) the second-stage cooling of small liquid droplets which were supercooled at

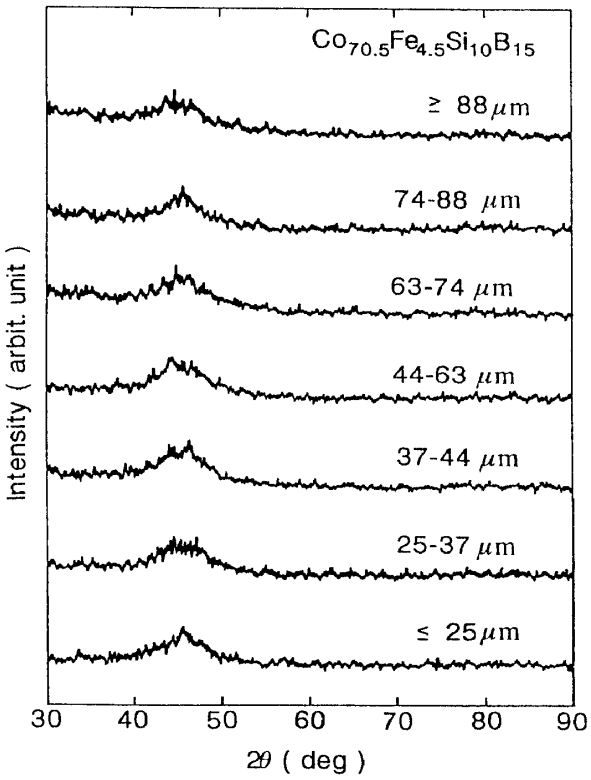

Fig. 6
X-ray diffraction patterns of flaky $Co_{70.5}Fe_{4.5}Si_{10}B_{15}$ powders produced by the two-stage quenching method. The data of spherical powders with a size fraction below 25 μm are also shown for comparison.

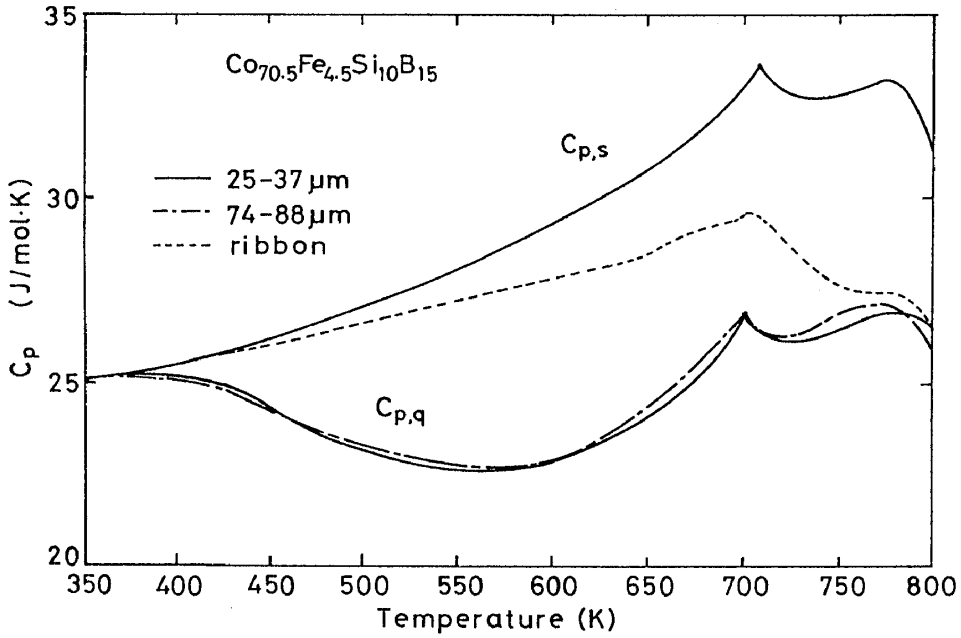

Fig. 7 The thermograms of flaky $Co_{70.5}Fe_{4.5}Si_{10}B_{15}$ amorphous powders with particle size fractions of 25-37 μm and 74-88 μm in the as-quenched state ($C_{p,q}$) and reheated state up to 800 K ($C_{p,s}$) produced by the two-stage quenching method. The data of the melt-spun amorphous ribbon are also shown for comparison.

temperatures below T_m, (2) the ultra-thinning of the powder thickness to 1 to 3 μm, and (3) the achievement of high thermal conductive state between the cooling rotator and the flaky powder resulting from the impingement at high kinetic energies.

As described above, the increase in cooling rate causes the significant increase in the production ratio of amorphous alloy powders. In addition, it has been reported[13] that the present new technique gives rise to the formation of an amorphous phase in new alloy systems in which an amorphous phase cannot be obtained by melt spinning as well as to the remarkable extension of glass-formation ranges in the alloy systems where the formation of an amorphous phase has previously been recognized. As an example, Fig. 8 shows the extension of the glass formation range in Fe-Si-C system by the use of the supercooled liquid quenching method. When the ribbon sample with a thickness of about 12 μm is prepared by melt spinning, the amorphous phase is formed only in the high solute concentration range above about 30 at% and no amorphous phase is formed in binary Fe-C alloys. On the other hand, when the supercooled liquid quenching technique is used, the formation range of the amorphous phase decreases to about 20 at%(Si+C), accompanied by the formation of the amorphous phase in the vicinity of the eutectic point (15 to 18 at%C) in Fe-C binary system.

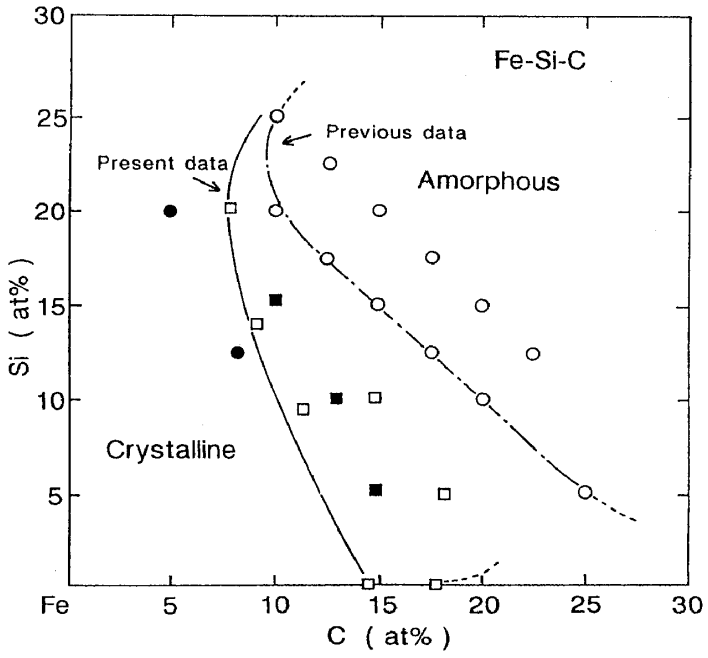

Fig. 8 Composition range for formation of an amorphous phase in Fe-Si-C alloys subjected to the two-stage quenching. The previous data of the glass formation range taken from Ref.14 are also shown for comparison.

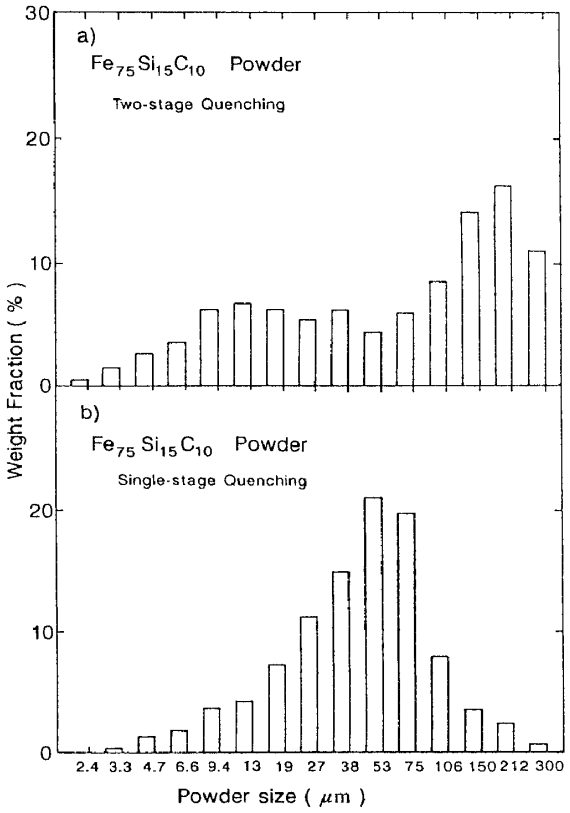

Fig. 9
Size distribution of $Fe_{75}Si_{15}C_{10}$ powders produced by impact flattening of atomized liquid droplets (a) and by high-pressure argon gas atomization (b).

It is expected that the particle size fraction of the atomized powders differs significantly between the conventional high-pressure gas atomization and the supercooled liquid quenching method. Figure 9 shows the distribution of particle size for $Fe_{75}Si_{15}C_{10}$ powders produced by both the methods[13]. The peak of the particle size fraction is located in the 38-75 μm range for the spherical powders produced by the high-pressure gas atomization and shifts to the 150-212 μm range for the flaky powders produced by the supercooled liquid quenching method, accompanying the significant decrease in the powder amount in the 38-75 μm size range. The contrastive change indicates that the flaky powders with the particle size of 150 to 212 μm are mainly produced by impact-flattening of the supercooled liquid droplets with a size fraction of 38-75 μm.

III. Expected Application Fields of Flaky Amorphous Alloy Powders

1. Application to magnetic filler materials

It is expected that the magnetic properties of the flaky amorphous powders with the unique morphology shown in Fig. 4 differ significantly in both the directions parallel and perpendicular to the

plane of the falky powder, leading to the appearance of significant anisotropy in magnetic properties. The composite materials in which $Co_{70.3}Fe_{4.7}Si_{10}B_{15}$ flaky powders and phenol resin were mixed at a weight ratio of 9:1 were produced by uniaxial pressing at 423 K. The resulting composites have a density of 4.1 to 4.4 Mg/m^3 and the falky powders in the composites lie preferentially along the direction perpendicular to the compressive applied load, as shown in Fig. 10. The orientation tendency tends to increase with increasing aspect ratio. Figure 11 shows the change in the B-H loop for the composites with powder size[15]. The magnetization is difficult for the composite made from the spherical powders with a size below 25 μm, leading to small saturation magnetization (B_s) and large coercivity (H_c). On the other hand, the magnetization becomes much easy for the composites made from the flaky powders, leading to the improvement of soft magnetic properties through the increase in B_s and the decrease in H_c. Furthermore, the improvement of the soft magnetic properties becomes significant with an increase of the aspect ratio, as shown in Fig. 11. B_{100}, μ_e at 1 kHz and H_c for the composite made from the 90-150 μm flaky powder are 2.6 kG, 550, 0.85 Oe, respectively, which are larger by 4.7 times for B_{100} and by 2.2 times for μ_e and smaller by 50 % for H_c as compared with the composite made from the spherical powder.

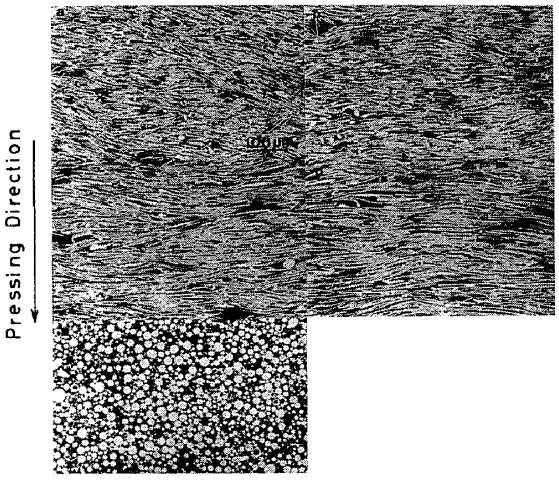

a : 25-45μm
b : 45-63μm
c : 63-90μm
d : 90-150μm
e : ≤25μm

Fig. 10
Optical micrographs showing the cross-sectional structure of $Co_{70.5}Fe_{4.5}Si_{10}B_{15}$ composites made from amorphous powders and phenol resin at a weight ratio of 9:1.

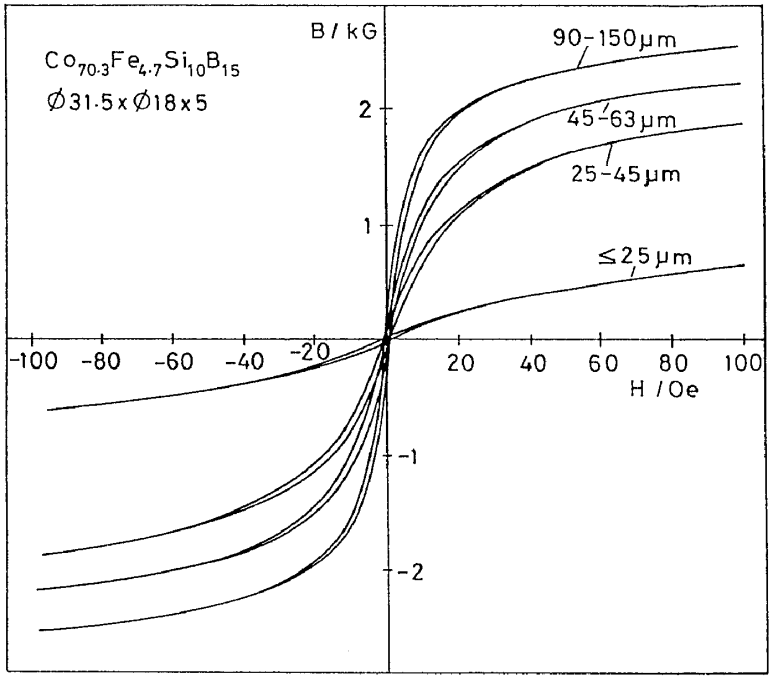

Fig. 11 Change in the B-H curve for the $Co_{70.3}Fe_{4.7}Si_{10}B_{15}$ composite core with powder particle size fraction.

These results indicate that the soft magnetic properties of the Co-base alloy composite increase significantly by the use of the flaky powder in comparison with those for the composite in which the spherical powder is used.

It has recently been found[16] that the nanoscale bcc phase obtained by crystallization of amorphous Fe-Zr-B phase has high μ_e values comparable to that for Co-Fe-Si-B amorphous alloys with zero magnetostriction and the B_s of the bcc phase is about 2.5 times higher than that for the Co-based amorphous phase. The high B_s value is particularly important in the application of the composites consisting of the flaky powder and phenol resin. The glass-forming ability of Fe-Zr-B alloys is lower than that of Co-Fe-Si-B alloys and hence no amorphous single phase is obtained in the spherical powders with a particle size below 25 μm produced by high-pressure Ar atomization. The application of the supercooled liquid quenching technique to Fe-Zr-B alloys has been found[17] to cause the formation of an amorphous single phase over the entire particle size fraction as shown in Fig. 12. Furthermore, Fig. 13 shows that the mostly single bcc phase with good soft magnetic properties is obtained by annealing the flaky amorphous powders for 3.6 ks at 923 K. The composite core produced by uniaxial hot-pressing the mixture of the bcc 90-150 μm flaky powders

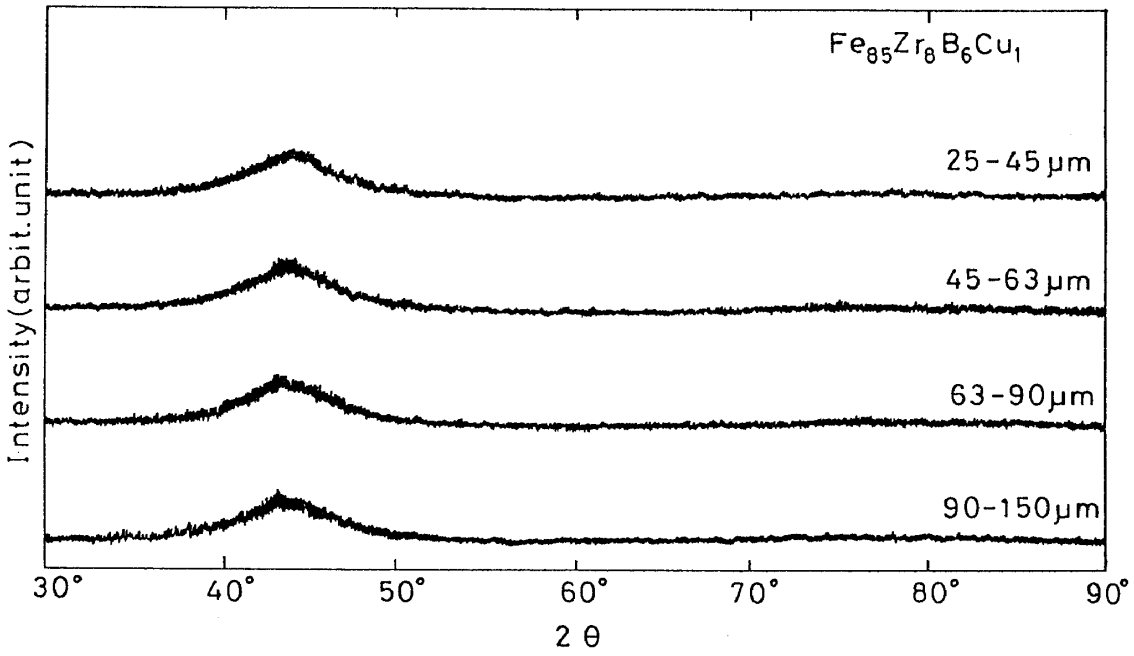

Fig. 12 X-ray diffraction patterns of $Fe_{85}Zr_8B_6Cu_1$ powders with different particle size fractions produced by the two-stage quenching method.

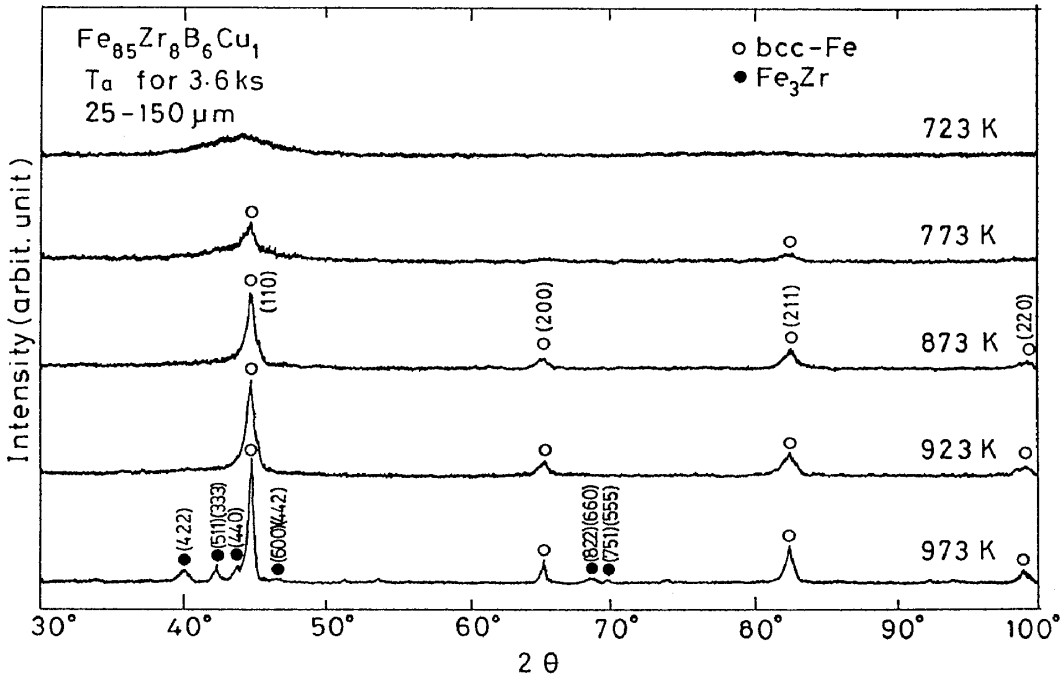

Fig. 13 Change in the X-ray diffraction pattern of the flaky $Fe_{85}Zr_8B_6Cu_1$ amorphous powders with annealing temperature in the case of annealing time of 3.6 ks.

and phenol resin with a mixing weight ratio of 9:1 exhibits soft magnetic properties of 5.4 kG for B_{100}, 500 for μ_e at 1 kHz and 1.2 Oe for H_c[17], as shown in Fig. 14. It is to be noticed that the B_{100} value is more than two times as high as that for the Co-Fe-Si-B composite core. The characteristics of 5.4 kG for B_s and 500 for μ_e are not obtained even for the composite cores made from amorphous Co-Fe-Si-B and Fe-Si-B flaky powders and hence the engineering importance of the flaky powders with the nonequilibrium bcc phase is hereafter expected to increase significantly.

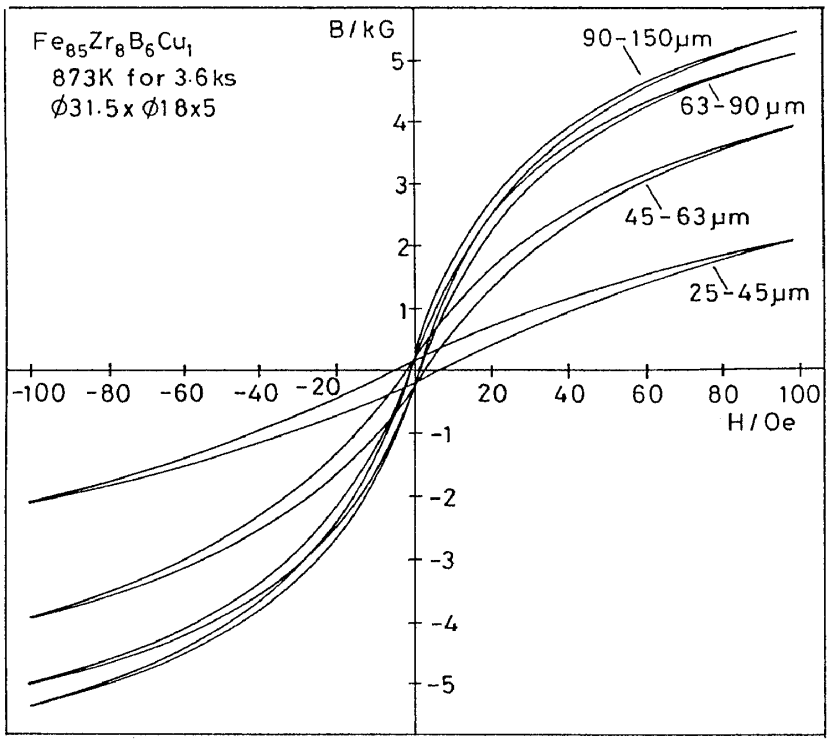

Fig. 14 B-H curves of the $Fe_{85}Zr_8B_6Cu_1$ composites made from bcc phase powders with different particle size fractions and phenol resin at a weight ratio of 9:1.

2. Application to corrosion-resistant coating materials

It is known that amorphous alloys in Fe-Cr-P-C[18] and Al-Ni-Mm[19] systems have corrosion resistance, tensile strength, hardness and wear resistance which exceed significantly those for the corresponding Fe- and Al-based crystalline alloys. Since the falky amorphous alloy powders do not contain any grain boundaries and have a very smooth

surface, the amorphous alloys have a low degree of scattering for light and ultraviolet rays, leading to considerably higher reflection ratios as compared with those for crystalline alloys. Furhermore, the flaky powder with the unique morphology shown in Fig. 4 is expected to have the labyrinth effect leadig to the highly dense and oriented packing states of the falky amorphous powders in painting chemical solution. The use of the falky powders in Fe-Cr-P-C and Al-Ni-Mm systems as coating materials aims at the utilization of the above-described features. As illustrated schematically in Fig. 15, the coating film made from the falky amorphous powders and chemical solution has been clarified[20] to have a number of characteristics such as high resistances against tensile and bending deformation and scratching damage, high reflection ratios against light and ultraviolet rays, good luster and high protectability resulting from the difficulty in the penetration of corrosive materials into metallic substrate based on the labyrinth effect. Here, it appears important to point out that the amorphous alloy powders with good corrosion resistance can be used even in water base solution where conventional crystalline alloy powders have not been used because of the poor corrosion resistance in the water base solution. If the use of organic solution is suppressed by the use of the flaky amorphous powder, the pollutional attack to the painting workers and the environmental pollution on earth are expected to be reduced. In the near future, the application of the amorphous flaky powders to coating materials is expected to be extended significantly.

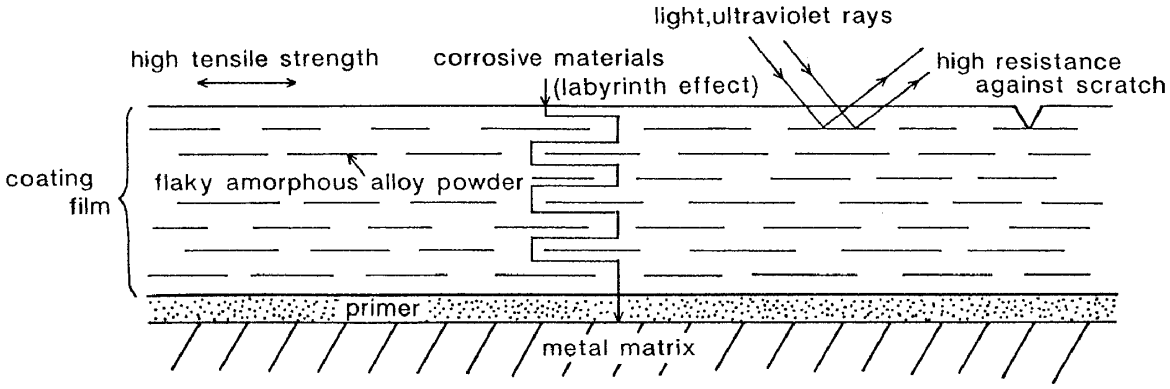

Fig. 15 Schematic illustration showing the internal structure and characteristics for the corrosion-resistant painting film using the flaky amorphous alloy powders as a coating material.

IV. Concluding Remarks

As described above, we succeeded in developing a new supercooled liquid quenching technique in which atomized supercooled liquid droplets with high flight velocities produced by high-pressure Ar atomization are flattened on a rapidly rotating wheel. Furthermore, the new quenching technique was found to cause the production of flaky amorphous powders with uniform and thin thickness of 1 to 3 μm. In addition, it has been clarified that the cooling rate obtained by the present new technique is considerably larger than those for the high-pressure gas atomization and the single-roller melt-spinning method and hence the resulting powders can be amorphized over the whole particle size fraction. No reference has been seen about the liquid quenching technique leading to the production of the unique flaky amorphous powders. In the near future, there is a high possibility that advanced materials with novel characteristics resulting from the formation of new nonequilibrium crystalline phase as well as from the amorphization in new alloy systems or at new alloy compositions are synthesized by utilizing the present new concept and technique of liquid quenching. Consequently, the present supercooled liquid quenching is expected to proceed as a new research field in rapidly solidified alloys.

References

1) N.J. Grant, Rapid Solidification Processing, Principles and Technologies, eds. R. Mehrabian, B.H. Kear and M. Cohen, Claitor's Publishing Division, Baton Rouge, LA (1977) p.230.
2) S.A. Miller and R.J. Murphy, Scripta Met., 13 (1979), 673.
3) A. Inoue, T. Masumoto, T. Ekimoto, S. Furukawa, Y. Kuroda and H.S. Chen, Met. Trans., 19A (1988), 235.
4) H. Ishii, M. Naka and T. Masumoto, Sci. Rep. RITU, A-29 (1981), 343.
5) I. Ohnaka, T. Fukusako and H. Tsutsumi, J. Japan Inst. Metals, 21 (1982), 1095.
6) A. Inoue, T. Komura, J. Saida, M. Oguchi, H.M. Kimura and T. Masumoto, Int. J. Rapid Solidification, 4 (1989), 181.
7) A. Inoue, J. Saida and T. Masumoto, Mater. Trans., JIM, 30 (1989), 359.
8) A. Inoue, J. Saida, Y. Tachiya, A.P. Tsai and T. Masumoto, MRS Int. Mtg. on Advanced Materials, 3 (1989), 359.

9) M. Oguchi, A. Inoue, H. Yamaguchi and T. Masumoto, Mater. Trans., JIM, 31 (1990), 1005.
10) M. Oguchi, A. Inoue and T. Masumoto, Mater. Sci. Eng., A133 (1991), 688.
11) H. Lubanska, J. Metals, 22 (1970), No.2, p.45.
12) J. Liu, L. Arnberg, N. Backstrom, H. Kalng and S. Savage, Powder Metall. Inst., 20 (1988), 589.
13) A. Inoue, J. Saida and T. Masumoto, Japan-US Cooperative Science Program Seminar on Solidification Processing of Advanced Materials, ed. T. Umeda (1989), p.131.
14) A. Inoue, S. Furukawa and T. Masumoto, Met. Trans., A18 (1987), 715.
15) M. Oguchi, Y. Harakawa, Y. Shimizu, A. Inoue and T. Masumoto, J. Japan Soc. of Powder and Powder Metallurgy, 38 (1991), 930.
16) K. Suzuki, A. Makino, N. Kataoka, A. Inoue and T. Masumoto, Mater. Trans., JIM, 32 (1991), 93.
17) M. Oguchi, Y. Harakawa, K. Suzuki, A. Inoue and T. Masumoto, unpublished research, (1992).
18) M. Naka, K. Hashimoto and T. Masumoto, J. Japan Inst. Metals, 38 (1974), 835.
19) A. Inoue, K. Ohtera and T. Masumoto, Sci. Rep. RITU, A35 (1990), 115.
20) M. Oguchi, Metals (1992), No.6, p.32.